polymers

MDPI

Article

Theoretical Study on Decomposition Mechanism of Insulating Epoxy Resin Cured by Anhydride

Xiaoxing Zhang [1,*], Yunjian Wu [1], Xiaoyu Chen [2], Hao Wen [1] and Song Xiao [1]

[1] School of Electrical Engineering, Wuhan University, Wuhan 430072, China; wuyunjian@whu.edu.cn (Y.W.); wenhao198711@163.com (H.W.); xiaosongxs@gmail.com (S.X.)
[2] State Grid Shaoxing Power Supply Company, Shaoxing 312000, China; xiaoyuwhu@163.com
* Correspondence: xiaoxing.zhang@outlook.com; Tel.: +86-1362-7275-072

Received: 11 July 2017; Accepted: 3 August 2017; Published: 4 August 2017

Abstract: High temperatures caused by partial discharge results in the decomposition of insulating epoxy resins in electrical equipment. In this paper, the ReaxFF force field is used to investigate the decomposition process of epoxy resins cured by anhydride and the formation mechanisms of small-molecule gases. Results show that the initiation reaction is the cleavage of an ester bond linked with an epoxy resin. Produced by the decomposition of ester groups, CO_2 is the first and most abundant product. Meanwhile, CH_2O can be generated through three main ways, although the process still depends on the decomposition of epoxy functional groups. H_2O is produced by free radical collision and dehydration. The production of small-molecule gases has the following sequence: CO_2, CH_2O, CO, and H_2O. The produced gases have the following order according to amount: CO_2, CH_2O, H_2O, and CO.

Keywords: anhydride; epoxy resin; decomposition; simulation

1. Introduction

Anhydride-cured epoxy resins are widely used as solid insulators in large electrical equipment because of their excellent resistance to leakage traces [1]. Despite these features, these resins are prone to defects such as grooves and gas gaps during their manufacture, transportation, and operation because of electric, heat, and mechanical stresses. These defects render the surface of epoxy resins vulnerable to partial discharge, which can lead to an average temperature rise of 170 °C and a maximum of 1000 °C around a volume of 5×10^{-11} cm^3 on the epoxy resin surface near the partial discharge area. Consequently, the epoxy resins are degraded. In particular, the surfaces of the epoxy resins become scabrous and gradually form grooves, thereby increasing the possibility of breakdown caused by the development of an electric tree in the epoxy resins [2–5]. Moreover, the products combine with water or oxygen in the equipment, thereby producing acidic substances, which not only dramatically increases surface conductivity but also speeds up the deterioration of epoxy resins [6,7]. Thus, studying the decomposition process of anhydride-cured epoxy resins is of great significance to the exploration of electric tree formation and the aging process of insulating resins.

There have been many researchers investigating the decomposition mechanism of epoxy resin [8,9] and the prevention of decomposition by enhancing its thermal conductivity [10,11]. Vlastara et al. [12] studied the decomposition process of epoxy resin cured by hexahydrophthalic anhydride heated with laser light. They found that the process produces large amounts of CO_2 and H_2O and certain amounts of acetylene, acetone, and other small volatile substances. Gao et al. [13] confirmed that gas generation occurs during the thermal aging process of epoxy-cast busbar. Hudon et al. [14–16] studied the liquid and solid matters formed on the surface of epoxy resins under partial discharge conditions, and subsequently determined that the solid matter is calcium oxalate.

The ReaxFF reactive force developed by Duin and Dasgupta et al. [17] defines the band angle and torsional force as a function of bond order and estimates the breakage between atoms on the basis of the relationship between bond length and bond order. Bond energy and bond order effectively simulate molecular reactions. The computational speed and accuracy of traditional quantum chemistry are sufficient for predicting the geometries, energies, and vibration energies of small molecules; however, these parameters are inadequate for exploring macromolecules and solid dynamic performance [18]. The ReaxFF force field can offset this disadvantage and has thus been widely used in small-molecule systems [19,20], polymer systems [21,22], high-energy material systems [23,24], metal oxide systems [25,26], and transition metal catalyst systems [27,28]. The thermal process of epoxy resin in printed circuit boards was investigated by ReaxFF force field. The first gas product was found to be CH_2O, and other main small-molecule products include H_2O, CO, and H_2 [29]. Zhang et al. simulated the decomposition process of epoxy resin heated by microwave by using ReaxFF, and they investigated the factors influencing the H_2O and H_2 production rates [30].

In this paper, the ReaxFF force field was used to analyze the thermal decomposition process of epoxy resin cured by acid anhydride at different angles. Several representative small-molecule gas products were then studied to produce a theoretical basis for the aging process and theory of solid insulation in electrical equipment.

2. Simulation Details

In this paper, three models of non-cross-linked epoxy resin were built. Module 1 contains one pure epoxy resin (PEP) molecule, which is formed by the dehydration condensation of two bisphenol A diglycidyl ether molecules, as shown in Figure 1a (①②③④⑤ represent the carbon-oxygen bonds). Module 2 consists of one molecule of epoxy resin cured by methyl hexahydrophthalic anhydride (EPMHA), as shown in Figure 1b. Module 3 contains 15 EPMHA molecules, as shown in Figure 1b.

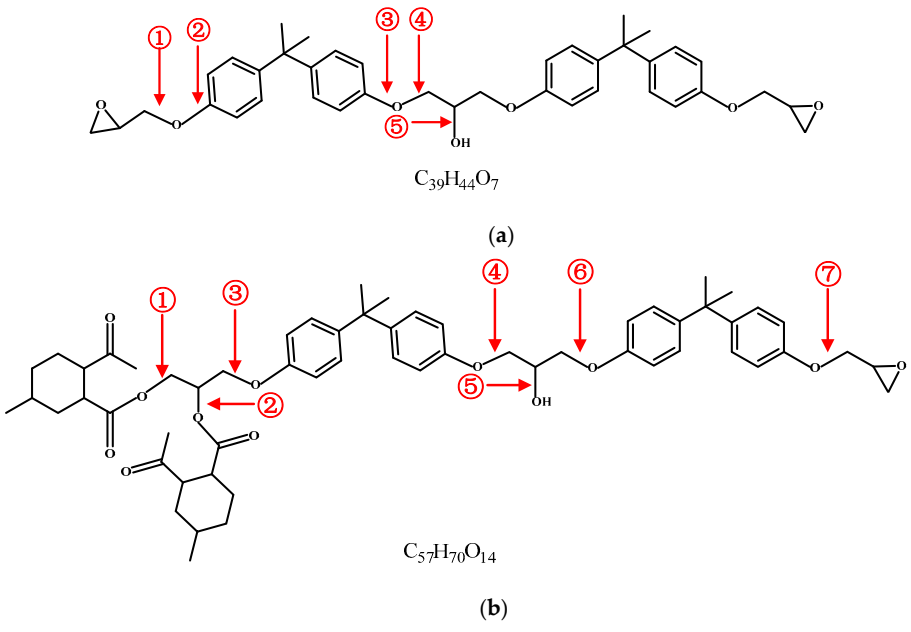

Figure 1. Structure of epoxy resin. (**a**) Structure of pure epoxy resin; (**b**) Structure of epoxy resin cured by anhydride.

The first step is to build three-dimensional periodic models, the initial densities of which were all set to 0.5 g/cm^3. Annealing via an iterative procedure was then performed, beginning with a molecular dynamics calculation by NVT ensemble at 600 K and then by NPT ensemble at 600 K and a constant pressure of 1.01 MPa (1 atm) for 100 ps; in the succeeding iterations, the temperature was

decremented by 50 °C and the process was repeated until the specified temperature for the dynamics was 300 K (around room temperature). After which, geometry optimization of 5000 iterations was performed to get a more stable structure. The final densities of the three models were 1.13, 1.13, and 1.17 g/cm^3 (Table 1). Subsequently, the NVT ensemble was selected, and the simulation temperature was set to 1300 K, which was the highest temperature during the real partial discharge. The time step and production time were then set to 0.1 fs and 1000 ps, respectively, to simulate the cook-off process.

Table 1. Model construction. EPMHA: epoxy resin cured by methyl hexahydrophthalic anhydride; PEP: pure epoxy resin.

Model	Material	Molecular formula	Number	Initial density g/cm^3	Final density g/cm^3
Model 1	PEP	$C_{39}H_{44}O_7$	1	0.5	1.13
Model 2	EPMHA	$C_{57}H_{70}O_{14}$	1	0.5	1.13
Model 3	EPMHA	$15*C_{57}H_{70}O_{14}$	15	0.5	1.17

The structures before and after the optimization of the three models are presented in Figure 2. Module 1 was used to study the process of PEP bond breakage under high temperatures, and the results were compared with the previous research results to verify the accuracy of the test program. Module 2 was used to simulate the bond-breaking process of EPMHA. The decomposition products of EPMHA during the cook-off process were obtained in Model 3. The decomposition mechanism of EPMHA and the formation of the corresponding products were analyzed by combining Models 2 and 3.

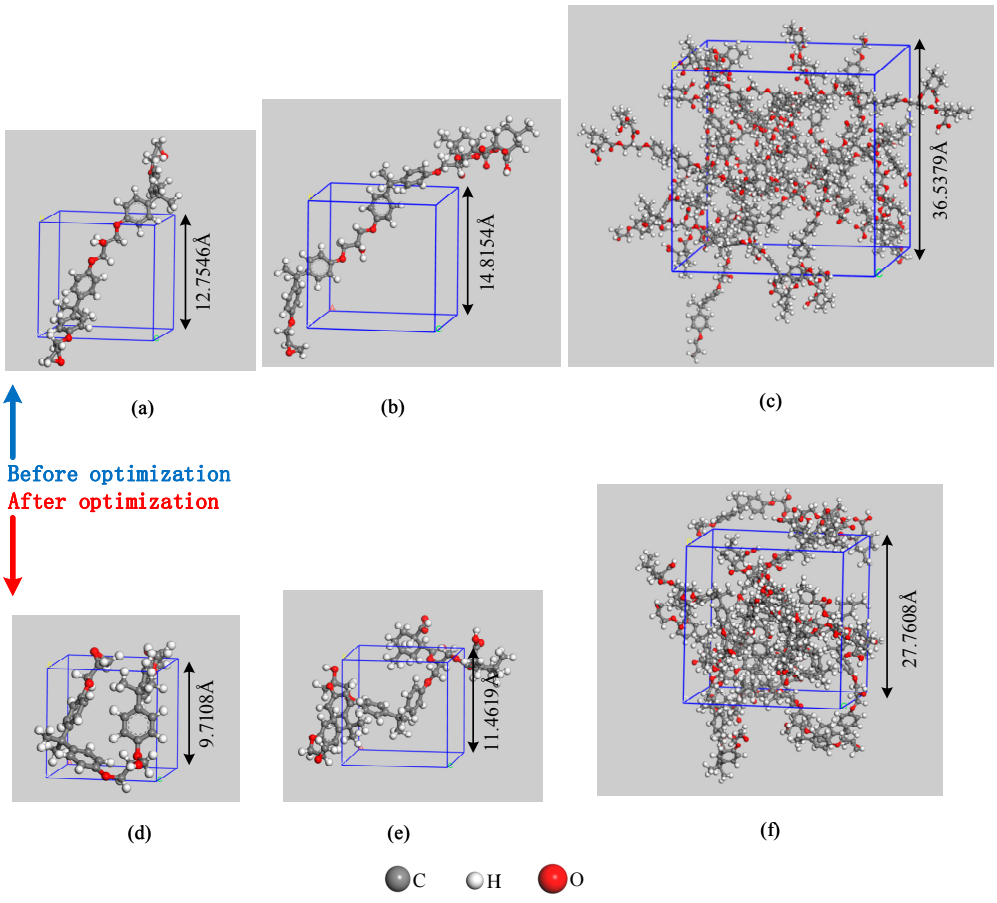

Figure 2. Structures of the three models. Structures before optimization of (**a**) Model 1, (**b**) Model 2, and (**c**) Model 3; Structures after optimization of (**d**) Model 1, (**e**) Model 2, and (**f**) Model 3.

3. Results and Discussion

3.1. Simulation Results of PEP

The carbon-oxygen bonds in epoxy resins tend to break, as shown in Figure 1a ①②③④⑤. According to Huckel's rule, parts with aromatic structures exhibit better thermal stability than those without, and the activation energy required for the fracture is higher, as shown in at Table 2. Thus, the ② and ③ carbon-oxygen bonds are difficult to fracture. Among ①④⑤, the ① carbon-oxygen bond has the lowest activation energy. Thus, the breaking of this bond likely initiates PEP decomposition as shown in Figure 3a, and then results in the production of unstable intermediate product, Group A, which turns into vinyl radical and formaldehyde. The next breakage is observed in the ④ carbon-oxygen bond. All these findings agree with the conclusion of the initiation reaction and first gas product of the decomposition of PEP [25].

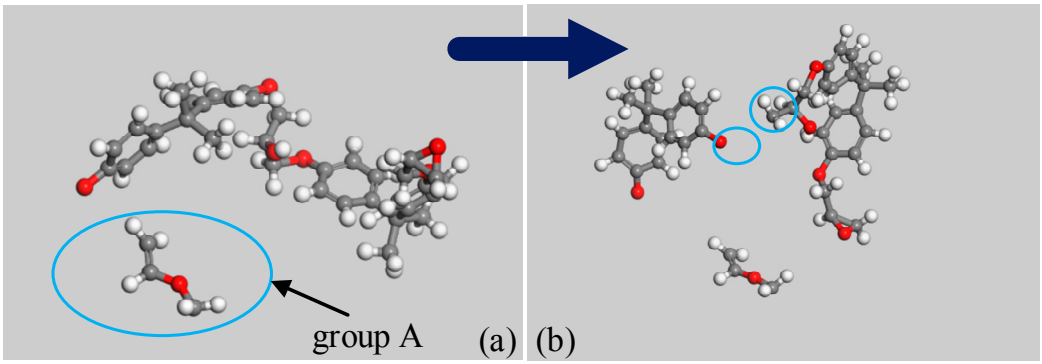

Figure 3. PEP decomposition process. (**a**) The first decomposition process; (**b**) The second decomposition process.

Table 2. Activation energy of some carbon-oxygen bonds.

Molecule	Breakage of bond	Activation energy (kJ/mol)
PEP	①	−232.64
	②	−332.53
	③	−320.62
	④	−261.75
	⑤	−276.54
EPMHA	①	−192.27
	②	−186.58
	③	−256.81
	④	−258.14
	⑤	−273.92
	⑥	−252.38
	⑦	−230.78

3.2. Simulation Results of EPMHA

Figure 4 shows the simulation results of Model 2. Figure 4b shows that the initiation reaction of EPMHA decomposition is the cleavage of ① and ② ester bonds. The reason is that the ester group linked with α-C and hydrogen atom linked with β-C are in the same plane under high temperatures. These components form a six-atom center that facilitates elimination. Thus, the breakage activation energy of ① and ② are the lowest, as shown in Table 2. As shown in Figure 4c, the first gas product is CO_2, and this result is consistent with the conclusion in this paper [8]. CO_2 is mainly derived from acyloxy groups in acid anhydride. The ⑦ carbon-oxygen bond (Figure 1b) then breaks and forms vinyl radical and formaldehyde (Figure 4d). This process is the main mode of formaldehyde production.

As shown in Figure 4e, the reaction produces free hydroxyl and free hydrogen because of the breakage of the ⑤ carbon-oxygen bond Figure 1b. The combination of free hydroxyl and hydrogen is one of the main approaches to producing H_2O. Figure 4f shows that propylene and bisphenol free radical appear in the system at the final simulation. Owing to the limitation of the simulation temperature and time, the epoxy resin molecules cannot decompose completely, and no hydrocarbon formation is observed

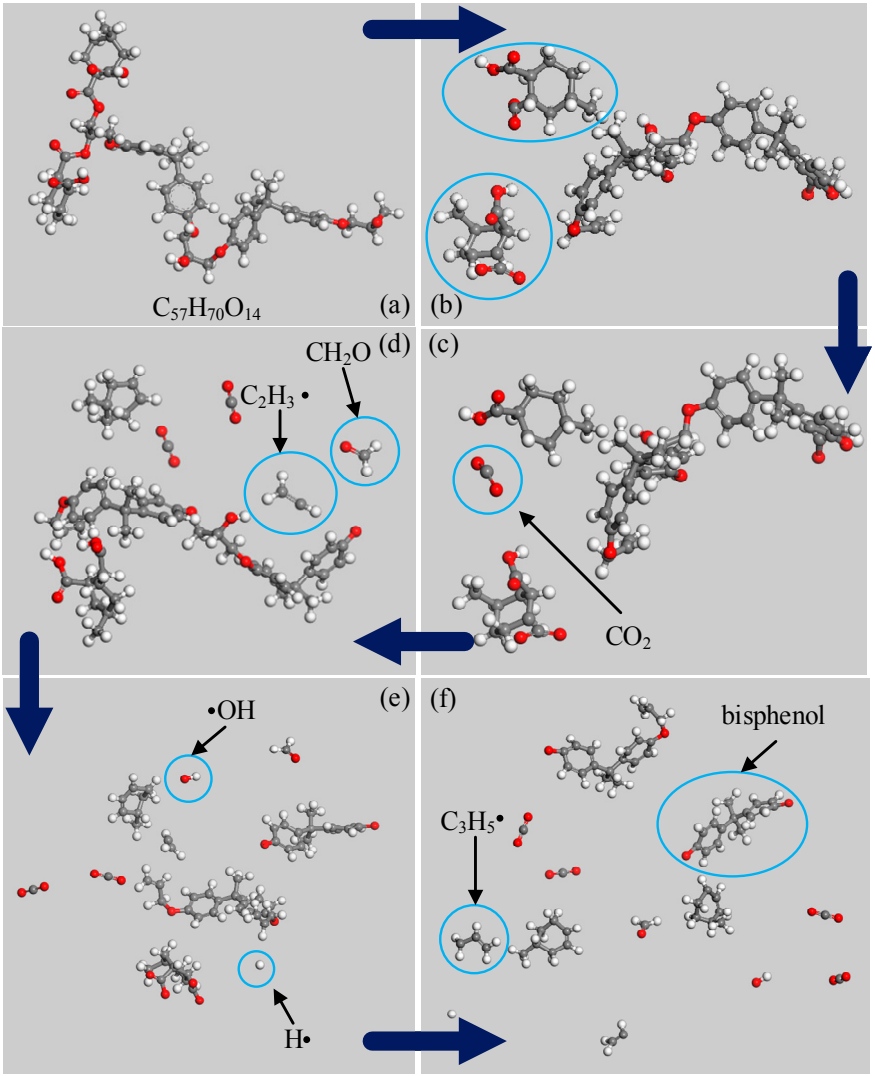

Figure 4. Decomposition process of EPMHA. (**a**) The first decomposition; (**b**) The second decomposition process; (**c**) The third decomposition process; (**d**) the forth decomposition process; (**e**) The fifth decomposition process; (**f**) The sixth decomposition process.

Figures 5 and 6 are the results of Model 3. The changes in compounds C_{57}, C_2, and C_3 over the simulation time is shown in Figure 5. C_{57} is a reactant. The main chain of the epoxy resin molecule starts to break from about 65 ps, and all the main chains of epoxy resin molecules are broken until 640 ps. The C_2 products mainly include ethylene radicals and acetaldehyde radicals, and the C_3 products contain propylene radicals, acetone radicals, acrolein radicals, propylene alcohol radicals, and so on.

Figure 6 shows the changes in CO_2, CH_2O, H_2O, and CO contents over the simulation time. The first gas product is CO_2 at about 70 ps, followed by CH_2O and H_2O. Thus, this result agrees with those of Model 2. The most abundant gas product is CO_2 because of the numerous acyloxy groups. The limitations in this paper include the simulation temperature and time result in a small amount

of CH_2O and H_2O, and the absence of H_2 and CH_4. The amount of hydroxyl groups in the model is comparable to the number of epoxy functional groups. However, the amount of CH_2O is larger than that of H_2O because the activation energy to form CH_2O is lower than that of H_2O.

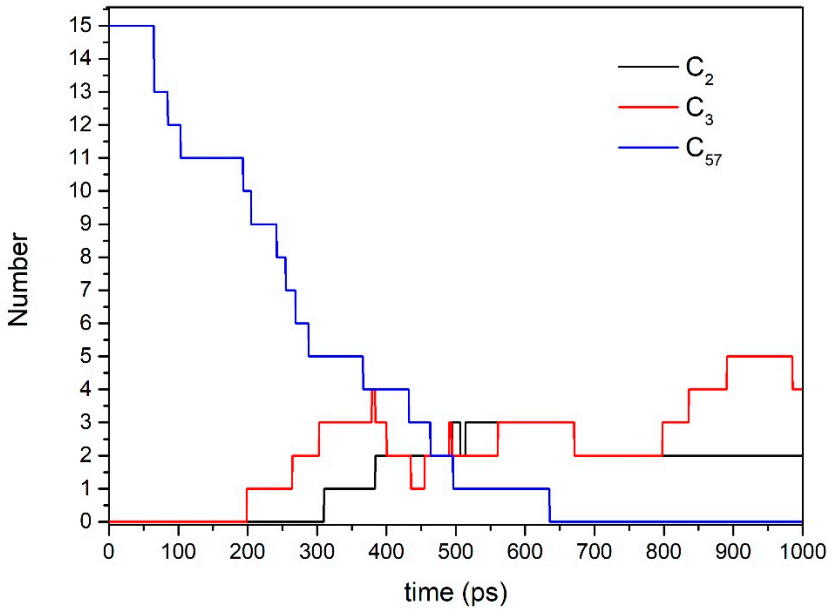

Figure 5. Time evolution of C_{57}, C_2, and C_3.

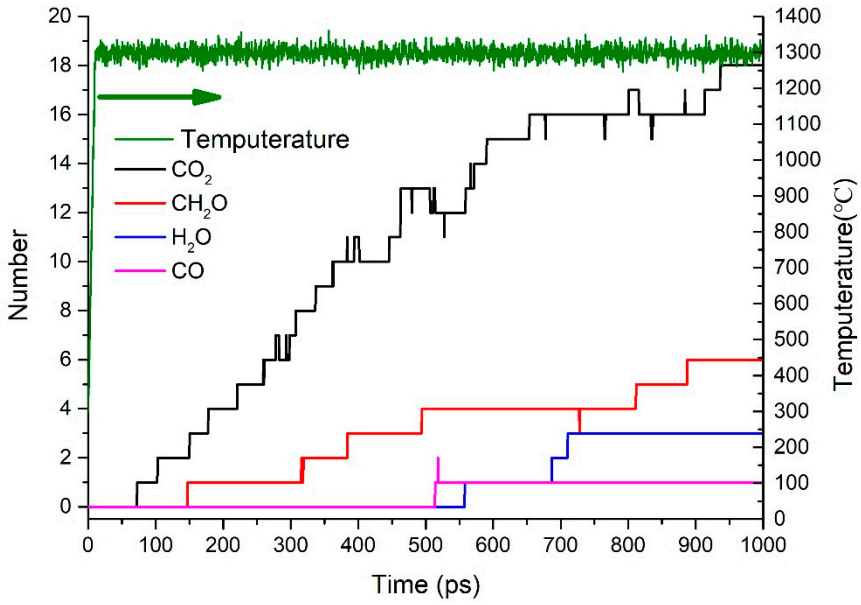

Figure 6. Time evolution of CO_2, CH_2O, H_2O, CO, and temperature.

3.3. Formation Mechanism of Gas Products

The main mechanism of CO_2 formation is p1~p3, as shown in Figure 7. The first step is the cleavage of the ester bond, followed by the removal of the acyloxy bond in the acid anhydride. Cycloolefin then forms. As shown in Figure 8 (p4~p6), CH_2O can be generated in three ways because the right-hand side of the ⑦ carbon-oxygen bond in Figure 1b can be converted through three different conversion methods. The water generation method includes three kinds. The p7 and p8 (Figure 9)

indicate that the intra-molecular elimination reaction produces water and intermolecular dehydration reaction, and p9 represents the water-producing collision of free radicals.

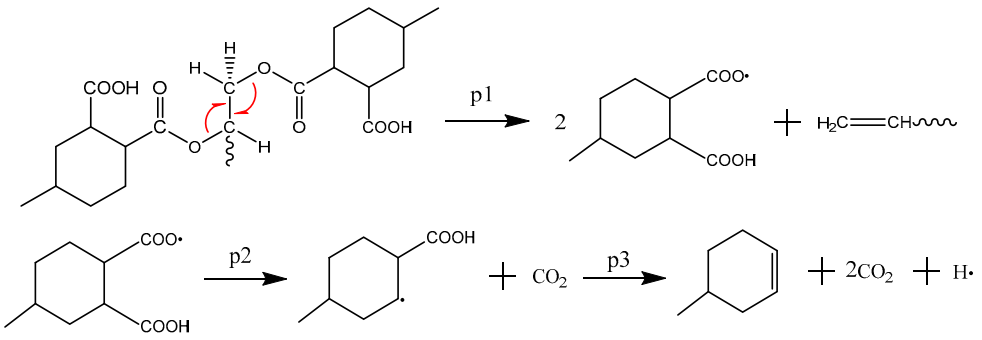

Figure 7. The main mechanism of CO_2 formation.

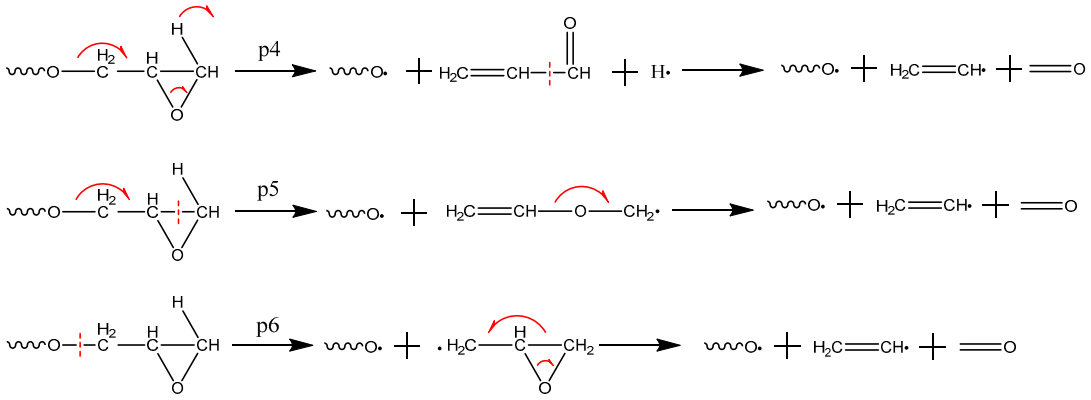

Figure 8. The main mechanism of CH_2O formation.

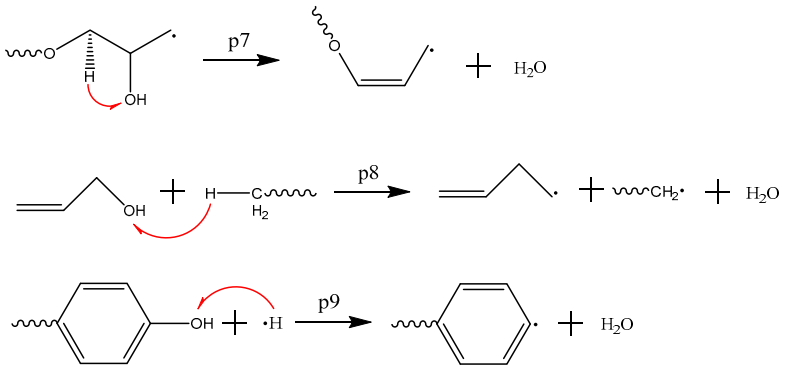

Figure 9. The main mechanism of H_2O formation.

4. Conclusions

In this paper, the ReaxFF force field was used to simulate a number of epoxy resin models, and the decomposition process of epoxy resin cured by anhydride and the formation path of main gas products were analyzed. The conclusions are as follows:

1. The initiation reaction of the decomposition of anhydride-cured epoxy resin is the cleavage of an ester bond;

2. The first and the most abundant product is CO_2. The other products were generated in the following sequence: CH_2O, CO, and H_2O. With respect to content, the following order was observed: CH_2O, H_2O, and CO.
3. CO_2 is produced from the carbonyl oxygen bond in anhydride; CH_2O, from the decomposition of epoxy functional group; H_2O, by free radical collision and dehydration.

Author Contributions: Xiaoxing Zhang and Yunjian Wu put forward the idea of the paper; Yunjian Wu, Xiaoyu Chen and Hao Wen designed and performed the simulation; Song Xiao analyzed the data; Xiaoxing Zhang and Yunjian Wu wrote the paper.

Conflicts of Interest: The authors declare no conflict of interest.

References

1. Uzunlar, E.; Schwartz, J.; Phillips, O.; Kohl, P.A. Decomposable and template polymers: Fundamentals and applications. *J. Electron. Packag.* **2016**, *138*, 15. [CrossRef]
2. Tang, J.; Liu, F.; Zhang, X.; Meng, Q.H.; Zhou, J.B. Partial discharge recognition through an analysis of SF6 decomposition products part 1: Decomposition characteristics of SF6 under four different partial discharges. *IEEE Trans. Dielectr. Electr. Insul.* **2012**, *19*, 29–36. [CrossRef]
3. Ju, T.; Xu, Z.R.; Zhang, X.X.; Sun, C.X. GIS partial discharge quantitative measurements using UHF microstrip antenna sensors, Electrical Insulation and Dielectric Phenomena. In Proceedings of the IEEE Conference on Electrical Insulation and Dielectric Phenomena (CEIDP 2007), Vancouver, BC, Canada, 14–17 October 2007. [CrossRef]
4. Champion, J.V.; Dodd, S.J. The effect of voltage and material age on the electrical tree growth and breakdown characteristics of epoxy resins. *J. Phys. D Appl. Phys.* **1995**, *28*, 398–407. [CrossRef]
5. Wu, K.; Dissado, L.A. Model for electrical tree initiation in epoxy resin. *IEEE Trans. Dielectr. Electr. Insul.* **2005**, *12*, 655–668.
6. Morshuis, P.H.F. Degradation of solid dielectrics due to internal partial discharge: some thoughts on progress made and where to go now. *IEEE Trans. Dielectr. Electr. Insul.* **2005**, *12*, 905–913. [CrossRef]
7. Sili, E.; Cambronne, J.P.; Naude, N.; Khazaka, R. Polyimide lifetime under partial discharge aging: Effects of temperature, pressure and humidity. *IEEE Trans. Dielectr. Electr. Insul.* **2013**, *20*, 435–442. [CrossRef]
8. Grassie, N.; Guy, M.I.; Tennent, N.H. Degradation of epoxy polymers: Part 1—Products of thermal degradation of bisphenol-A diglycidyl ether. *Polym. Degrad. Stab.* **1985**, *12*, 65–91. [CrossRef]
9. Grassie, N.; Guy, M.I.; Tennent, N.H. Degradation of epoxy polymers: 2—Mechanism of thermal degradation of bisphenol-A diglycidyl ether. *Polym. Degrad. Stab.* **1985**, *13*, 11–20. [CrossRef]
10. Zhang, Y.H.; Choi, J.R.; Park, S.J. Thermal conductivity and thermo-physical properties of nanodiamond-attached exfoliated hexagonal boron nitride/epoxy nanocomposites for microelectronics. *Compos. Part A Appl. Sci. Manuf.* **2017**, *101*, 227–236. [CrossRef]
11. Zhang, Y.; Rhee, K.Y.; Park, S.J. Nanodiamond nanocluster-decorated graphene oxide/epoxy nanocomposites with enhanced mechanical behavior and thermal stability. *Compos. Part B* **2017**, *114*, 111–120. [CrossRef]
12. Vlastaras, A.S. Thermal degradation of an anhydride-cured epoxy resin by laser heating. *J. Phys. Chem.* **1970**, *74*, 2496–2501. [CrossRef]
13. Gao, N.; Zhang, W.; Liu, Z.; Huang, K.F.; Jin, H.Y.; Wu, C. Study on thermal aging characteristics of epoxy resin/inorganic filler composites for the fully casting bus bar, Electrical Insulation and Dielectric Phenomena. In Proceedings of the 2013 IEEE Conference on Electrical Insulation and Dielectric Phenomena (CEIDP), Shenzhen, China, 20–23 October 2013. [CrossRef]
14. Hudon, C.; Bartnikas, R.; Wertheimer, M.R. Chemical and physical degradation effects on epoxy surfaces exposed to partial discharges. In Proceedings of the International Conference on Properties and Applications of Dielectric Materials, Brisbane, Australia, 3–8 July 1994. [CrossRef]
15. Hudon, C.; Bartnikas, R.; Wertheimer, M.R. Effect of physico-chemical degradation of epoxy resin on partial discharge behavior. *IEEE Trans. Dielectr. Electr. Insul.* **1995**, *2*, 1083–1094. [CrossRef]
16. Hudon, C.; Bartnikas, R.; Wertheimer, M.R. Surface conductivity of epoxy specimens subjected to partial discharges. In Proceedings of the Conference Record of the 1990 IEEE International Symposium on Electrical Insulation, Toronto, ON, Canada, 3–6 June 1990. [CrossRef]

17. Van Duin, A.C.T.; Dasgupta, S.; Lorant, F.; Iii, W.A.G. ReaxFF: A Reactive force field for hydrocarbons. *J. Phys. Chem. A* **2001**, *105*, 9396–9409. [CrossRef]
18. Chenoweth, K.; van Duin, A.C.T.; Goddard, W.A. ReaxFF reactive force field for molecular dynamics simulations of hydrocarbon oxidation. *J. Phys. Chem. A* **2008**, *112*, 1040. [CrossRef] [PubMed]
19. Mueller, J.E.; van Duin, A.C.T.; Goddard, W.A. Application of the ReaxFF reactive force field to reactive dynamics of hydrocarbon chemisorption and decomposition. *J. Phys. Chem.* **2010**, *114*, 5675–5685. [CrossRef]
20. Agrawalla, S.; van Duin, A.C.T. Development and application of a ReaxFF reactive force Field for hydrogen combustion. *J. Phys. Chem. A* **2011**, *115*, 960–972. [CrossRef] [PubMed]
21. Chenoweth, K.; Cheung, S.; van Duin, A.C.T.; Iii, W.A.G.; Kober, E.M. Simulations on the thermal decomposition of a poly(dimethylsiloxane) polymer using the ReaxFF reactive force field. *J. ACS* **2005**, *127*, 7192–7202. [CrossRef] [PubMed]
22. Ballistreri, A.; Garozzo, D.; Montaudo, G. Mass spectral characterization and thermal decomposition mechanism of poly(dimethylsiloxane). *Macromolecules* **2015**, *191*, 1. [CrossRef]
23. Chang, J.; Lian, P.; Wei, D.Q.; Chen, X.R.; Zhang, Q.M.; Gong, Z.Z. Thermal decomposition of the solid phase of nitromethane: ab initio molecular dynamics simulations. *Phys. Rev. Lett.* **2010**, *105*, 188302. [CrossRef] [PubMed]
24. Guo, F.; Zhang, H.; Cheng, X.L. Molecular dynamic simulations of solid nitromethane under high pressures. *J. Theor. Comput. Chem.* **2010**, *9*, 315–325. [CrossRef]
25. Raymand, D.; van Duin, A.C.; Baudin, M.; Hermansson, K. A reactive force field (ReaxFF) for zinc oxide. *Surf. Sci.* **2008**, *602*, 1020–1031. [CrossRef]
26. Chenoweth, K.; van Duin, A.C.T.; Persson, P.; Cheng, M.J.; Oxgaard, J.; Iii, W.A.G. Development and application of a ReaxFF reactive force field for oxidative dehydrogenation on vanadium oxide catalysts. *J. Phys. Chem. A* **2008**, *112*, 14645–14654. [CrossRef]
27. Nielson, K.D.; van Duin, A.C.; Oxgaard, J.; Deng, W.Q.; Iii, W.A.G. Development of the ReaxFF reactive force field for describing transition metal catalyzed reactions, with application to the initial stages of the catalytic formation of carbon nanotubes. *J. Phys. Chem. A* **2005**, *109*, 493. [CrossRef] [PubMed]
28. Iii, W.A.G.; Mueller, J.E.; Chenoweth, K.; van Duinc, A.C.T. ReaxFF Monte Carlo reactive dynamics: application to resolving the partial occupations of the M1 phase of the MoVNbTeO catalyst. *Catal. Today* **2010**, *157*, 71–76.
29. Diao, Z.J.; Zhao, Y.M.; Chen, B.; Duan, C.L.; Song, S. ReaxFF reactive force field for molecular dynamics simulations of epoxy resin thermal decomposition with model compound. *J. Anal. Appl. Pyrolysis* **2013**, *104*, 618–624. [CrossRef]
30. Zhang, Y.M.; Li, J.L.; Wang, J.P.; Yang, X.S.; Shao, W.; Xiao, S.Q.; Wang, B.Z. Research on epoxy resin decomposition under microwave heating by using ReaxFF molecular dynamics simulations. *RSC Adv.* **2014**, *4*, 17083–17090. [CrossRef]

© 2017 by the authors. Licensee MDPI, Basel, Switzerland. This article is an open access article distributed under the terms and conditions of the Creative Commons Attribution (CC BY) license (http://creativecommons.org/licenses/by/4.0/).